Progress In Electromagnetics Research B, Vol. 54, 203–225, 2013

DESIGN OF DEFECTED GROUND BAND PASS FILTERS USING STEPPED IMPEDANCE RESONATORS

Shraddha Sharma[1], Raj Kumar[2], Raghupatruni V. S. R. Krishna[3, *], and Rajas Khokle[3]

[1]PICT, Pune, India

[2]ARDE, Pune, India

[3]DIAT, Pune, India

Abstract—In this paper, band-pass filters based on the microstrip configuration and utilizing coupled defected ground structures are presented. The 50 Ω microstrip line has a gap discontinuity in the middle and characterized by stepped impedance resonators on either half. The four fractal geometries tested for defected ground are the first and second iterations of the modified Moore curve, the closed staircase curve and a dual concentric closed staircase curve. The filters have a compact size and planar geometry. The modified Moore first iteration has a measured pass band from 2.27 GHz to 11.86 GHz, whereas the second iteration has a measured pass band from 1.85 GHz to 6.71 GHz. The measured pass band of the closed staircase filter is from 2.38 GHz to 7.21 GHz. The dual-concentric closed-staircase DGS filter offers a dual-band response with the measured pass band being from 2.41 GHz to 5.01 GHz and from 5.81 GHz to 8.35 GHz. All the filters can have applications in the UWB region. A parametric study showing the effect of the various controlling parameters is also presented.

1. INTRODUCTION

For the short range wireless applications, such as UWB communication, medical imaging and centimeter precision range measurements, the Federal Communications Committee (FCC) allocated the unlicensed frequency band from 3.1 GHz to 10.6 GHz in February 2002. In many microwave and millimeter wave systems, the filters are the

Received 9 July 2013, Accepted 28 August 2013, Scheduled 5 September 2013

* Corresponding author: Raghupatruni V. S. Ram Krishna (rk_nedes@yahoo.co.in).

critical components. Consequently, the UWB filter is one of the most important parts of the UWB wireless communication system. The planar UWB filters are used to select or reject certain band of frequencies, suppress harmonics and spurious signals of the amplifiers and oscillators. The microstrip filter designed by using stepped impedance resonators is one of the ways of obtaining an ultra-wideband response. However, the main disadvantage of such a filter is the existence of harmonics and poor power handling capability. In order to overcome these disadvantages, new techniques are investigated. The Defected Ground Structure (DGS) as an Electromagnetic Band Gap (EBG) is one of such novel and effective techniques to improve the response of low pass filters and band-pass filters [1]. A defected ground structure for the microstrip transmission line has etched-slots, i.e., defects in a metallic ground plane which disturbs the current distribution and thus alters the response of the filter [2]. The defected ground structure introduces inductance and capacitance which provides the rejection bands in the filter output. Further, the DGS technology can be used to reduce the size of the microwave circuit. Because of these characteristics, DGS are increasingly used in designing microwave circuits.

There are different DGS shapes, such as spiral shape, C-shape, Dumbbell shape, H-shape, circular slot, open loop, close loop shapes which can be used in the metallic ground plane to design the filter circuits. In [2], a Von Koch fractal DGS is proposed for the realization of the band-pass filter. In [3], a split ring resonator (SRR) as a defected ground structure is proposed, and band-pass filter with reduced size is designed. However, due to the compactness provided by fractal shapes, the demand for fractal technology is increasing day by day in antenna as well as in filters [4–10], due to the fact that the electrical length of the structure increases with iteration while the structure maintains a self-similarity with previous iteration.

The Hilbert fractal with its self similar and space filling nature can be a suitable candidate for the miniaturization of the filter. A loop version of Hilbert curve is given by E. H. Moore, aptly known as Moore Curve. A modified version of Moore curve to obtain a closed loop structure is proposed in this paper. In addition to the modified Moore curve, another closed curve for defected ground structure is also proposed. This curve resembles a staircase and so named as closed staircase structure. In Section 2, the generation of the modified Moore curve and the closed staircase is explained followed by the design and geometry of the proposed filters in Section 3. The results of the proposed filters are discussed in Section 4, and a detailed parametric analysis is given in Section 5.

2. GENERATION OF CURVES

2.1. Hilbert Fractal and Modified Moore Fractal Curves

There are different fractal shapes which are used to miniaturize the components like antennas and filters. One such fractal curve is Hilbert Curve, first introduced by David Hilbert. Apart from being self-similar, this curve also has space-filling property, which means that after several iterations the curve completely fills the space. Consequently, for such a family of space filling curves the Housdorff dimension is 2.

In [3], we have the equation for the above fractal curve which is fitted in a square section having side given by 'G'. For creating this curve, first a square of size G, called grid, is divided into four equal parts, and the centers of these four parts are joined to get a U shape. This is zeroth iteration. Next, each part is further divided into four parts, i.e., the grid is divided into 16 parts. The copies of the lower half are kept the same whereas those of upper half are rotated 90°. The four sections are connected to each other by additional 3 lines. This procedure is repeated for higher iterations. The total number of lines in the curve in terms of iteration is given by Equation (1) while the length of each section is given by Equation (2). Total length of the curve is thus given by Equation (3) which is also known as Euclidean length.

$$\text{No. of sections} = 2^{2(j+1)} - 1 \quad \text{for} \quad j = 0, 1, 2, 3, \ldots \tag{1}$$

$$\text{Length of each section} = \frac{G}{2^{(j+1)}} \quad \text{for} \quad j = 0, 1, 2, 3, \ldots \tag{2}$$

$$\therefore H\left(L_{Total_j}\right) = G\left(2^{(j+1)} - \frac{1}{2^{(j+1)}}\right) \quad \text{for} \quad j = 0, 1, 2, 3, \ldots \tag{3}$$

This conventional Hilbert curve is an open ended curve. In order to couple energy efficiently from one port to another, closed structures may be more suitable. For this, a loop version of the Hilbert curve known as 'Moore curve' (after E. H. Moore) can be used. This curve can be obtained by the union of the four copies of the Hilbert curve such that their end points coincide. This curve is slightly modified by closing the loop so formed and by rotating it 90°. The first 3 iterations of Hilbert curve, Moore curve and modified Moore curve are shown in Figure 1. It can be noted that for modified Moore fractal, the total number of line sections will be one more than conventional Hilbert or Moore curve. Consequently, the total length will also be more. The total number of parts and total length for jth iteration of the modified Moore curve ($MM(l_{Total_j})$) can be given by Equations (4) & (5). It can be noted that the length of each section is still given by Equation (2).

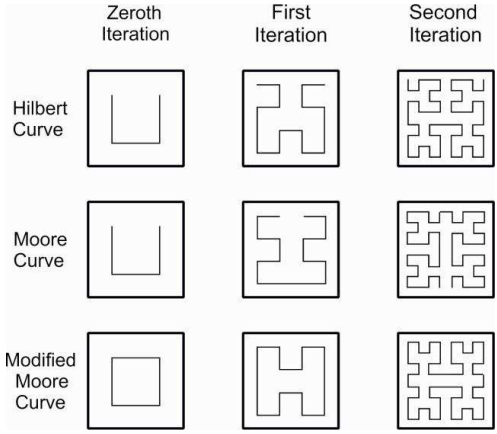

Figure 1. Zeroth, first and second iterations of hilbert, moore and modified moore fractals.

From Equations (3) & (5), the difference of Euclidean length between Hilbert curve and the proposed modified Moore curve Δl_j is given by Equation (6). From Equation (6), it can be seen that as the number of iterations goes on increasing, the difference in length falls off rapidly.

$$\text{No. of Parts} = 2^{2(j+1)} \quad \text{for} \quad j = 0, 1, 2, 3, \ldots \tag{4}$$

$$MM(l_{Total_j}) = G \cdot 2^{(j+1)} \quad \text{for} \quad j = 0, 1, 2, 3, \ldots \tag{5}$$

$$\Delta l_j = MM(l_{Total_j}) - H(l_{Total_j}) = \frac{G}{2^{(j+1)}} \quad \text{for} \quad j = 0, 1, 2, 3, \ldots \tag{6}$$

2.2. Closed Staircase Curve

Consider a square arranged diagonally as shown to the extreme left in Figure 2. Let 'x' be the length of one side. This can be considered as zeroth iteration. For the first iteration, each side is divided into 3 equal parts. For the second iteration, it is divided into 5 equal parts. Subsequently for the jth iteration, each side is divided into $(2j + 1)$ equal parts. From the first part, a line at an angle of $+45°$ from left end and $135°$ from the right end is drawn. From the second part, a line at an angle of $-45°$ from left end and $-135°$ from the right end is drawn. These steps are repeated again for the further parts to get the proposed staircase-like structure. Zeroth, first, second and third iterations of the proposed curve are shown in Figure 2.

The length of dimension 'y' can be taken as a characteristic for defining this curve. By using simple geometric relations, 'y' can be represented in terms of the length of one side of the zeroth iteration

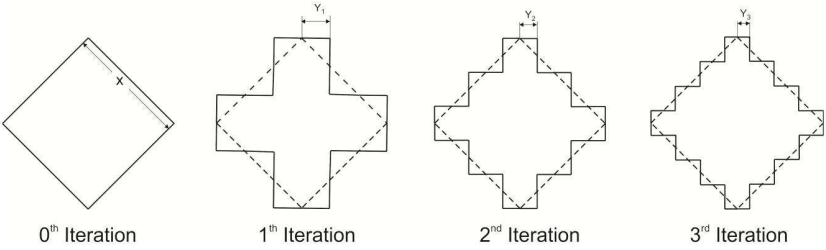

Figure 2. Iterations of proposed closed staircase structure.

('x') to form a defining Equation (7). The total length of the curve so formed can be given by Equation (8). It can be seen that even though the number of iterations goes on increasing the total length of the curve remains the same except for zeroth iteration.

$$y_{(j)} = \frac{1}{\sqrt{2}} \frac{x}{(2j+1)} \quad \text{for} \quad j = 1, 2, 3, 4, \ldots \tag{7}$$

$$l_{tot_j} = \begin{cases} 4x & \text{for} \quad j = 0 \\ 4 \times \sqrt{2}x & \text{for} \quad j = 1, 2, 3, \ldots \end{cases} \tag{8}$$

Since the total length remains the same, it is expected that the lowest frequency of operation will remain the same; however since the steps go on increasing, the current distribution will change, and it is expected to increase the bandwidth.

3. DESIGN OF PROPOSED STRUCTURE

The proposed filters are simulated using CST Microwave studio and designed on Rogers 5880 substrate with dielectric constant 2.2, thickness 0.508 mm and $\tan\delta = 0.0009$. The stepped impedance resonators (SIR) on the top microstrip plane are capacitively coupled by a spacing, i.e., (S) of 0.2 mm. Figure 3 also shows the different geometries traced by the slot of width $Wd = 0.2$ mm on the ground plane.

Figures 3(a) and 3(b) show the 1st and 2nd iterations of the modified Moore curve filters. The original grid size for making the 1st and 2nd iterations of the modified Moore fractal is 20 mm × 20 mm. So, the total size of the filter is 20 mm × 20 mm. The SIR on the top plane is suitably modified for impedance matching to get the passband below −10 dB.

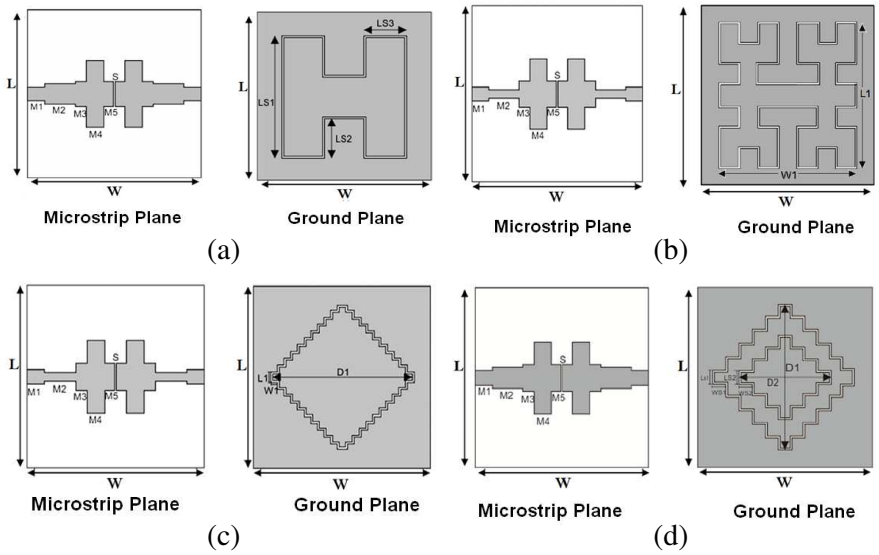

Figure 3. (a) Modified moore curve filter (1st iteration). (b) Modified moore curve filter (2nd iteration). (c) Closed staircase curve filter. (d) Dual concentric closed staircase curve filter.

After a detailed parametric study of various iterations of the closed staircase structure (discussed in Section 5.2), the 11th iteration is fabricated and tested. For obtaining dual-band response, the dual-concentric curve is designed and tested. The outer curve has the 5th iteration whereas inner curve has the 3rd iteration. Figures 3(c) and 3(d) show the top and ground planes of the Closed Staircase DGS (CS-DGS) filter and Dual-Concentric Closed Staircase DGS (DCCS-DGS) filter. The total size of both filters is 20 mm × 20 mm. The value of 'x' for CS-DGS filter is $8\sqrt{2}$ mm thereby making $D1 = 16$ mm. Similarly, for DCCS-DGS, $D1$ and $D2$ are 16 mm and 10.5 mm for outer and inner curves, respectively. All other dimensions shown in Figure 3 are detailed in Table 1.

Following [11–14], an equivalent circuit for the proposed band-pass filters based on the stepped impedance resonator configuration and utilizing the defected ground structure is shown in Figure 4. Each half plane of the filter has a SIR modeled as a T-circuit and a series R-L-C circuit to represent the fractal DGS section on that half. The gap discontinuity at the center is also accounted for in the equivalent circuit. Photographs of the fabricated filters are shown in Figures 5 & 6.

Table 1. Dimensions of the proposed filter structures.

Modified Moore First Iteration												
Label	M1		M2		M3		M4		M5		$LS1$	$LS2$=$LS3$
Parameter	$L1$	$W1$	$L2$	$W2$	$L3$	$W3$	$L4$	$W4$	$L5$	$W5$		
Value (mm)	2	1.6	3.5	2.4	1.3	3	2	8	1.1	3	15	5
Modified Moore Second Iteration												
Label	M1		M2		M3		M4		M5		$L1$	$W1$
Parameter	$L1$	$W1$	$L2$	$W2$	$L3$	$W3$	$L4$	$W4$	$L5$	$W5$		
Value (mm)	2	1.6	3.5	1	1.3	3	2	8	1.1	3	17.5	17.5
Closed Staircase Structure												
Label	M1		M2		M3		M4		M5		$L1$	$W1$
Parameter	$L1$	$W1$	$L2$	$W2$	$L3$	$W3$	$L4$	$W4$	$L5$	$W5$		
Value (mm)	2	1.6	3.5	1.1	1.3	3	2	8	1.1	3	1.5	1.5
Dual Concentric Closed Staircase Structure												
Label	M1		M2		M3		M4		M5		$LS1$=LS2	$LS2$=$WS2$
Parameter	$L1$	$W1$	$L2$	$W2$	$L3$	$W3$	$L4$	$W4$	$L5$	$W5$		
Value (mm)	2	1.6	3.5	2.4	1.3	3	2	8	1.1	3	1.5	1.5

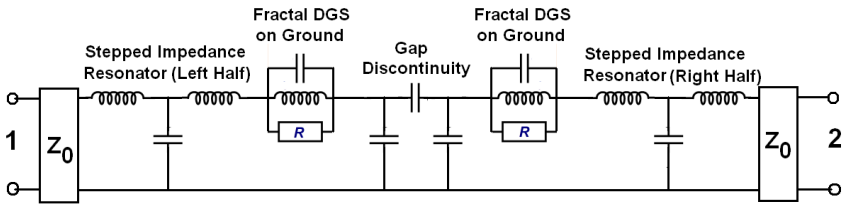

Figure 4. Equivalent circuit for the proposed SIR-DGS filters.

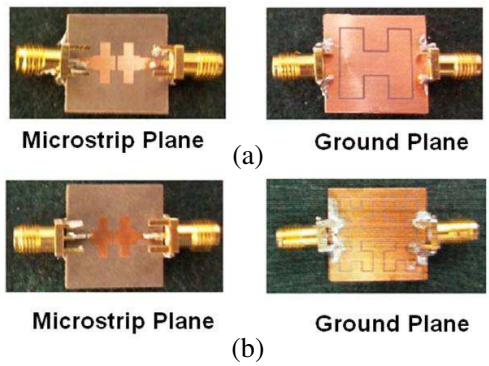

Figure 5. Photograph of the fabricated filters. (a) Modified moore — 1st iteration. (b) Modified moore — 2nd iteration.

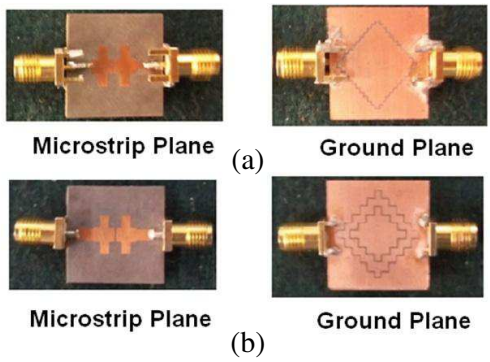

Figure 6. Photograph of the fabricated filters. (a) Closed staircase. (b) Dual concentric closed staircase.

4. SIMULATED AND MEASURED RESULTS

The filters are tested using a two-port R&S Vector Network Analyzer ZVA Z40. Comparisons of simulated and experimental S_{11} and S_{21} for the 1st and 2nd iterations of modified Moore fractal are shown in Figures 7 and 8, respectively, while those for CS-DGS and DCCS-DGS filters are shown in Figures 9 & 10, respectively. The simulated and measured lowest frequency (F_L), highest frequency (F_H), bandwidth and average insertion loss in passband (-10 dB) for the modified Moore filters are given in Table 2 while those for CS-DGS and DCCS-DGS are given in Table 3.

It can be seen from Table 2 that as the iteration increases for the Moore filters, the lowest frequency of operation decreases. Thus

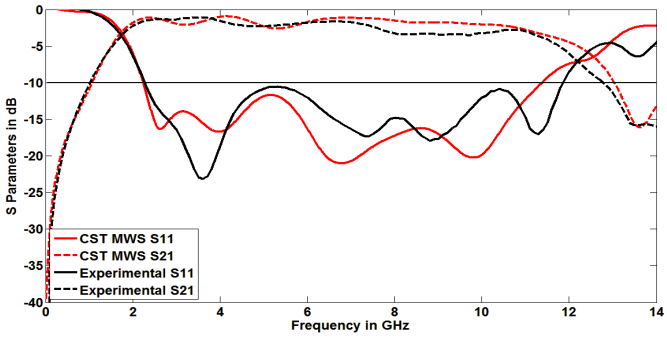

Figure 7. Simulated and experimental results of modified moore first iteration DGS filter.

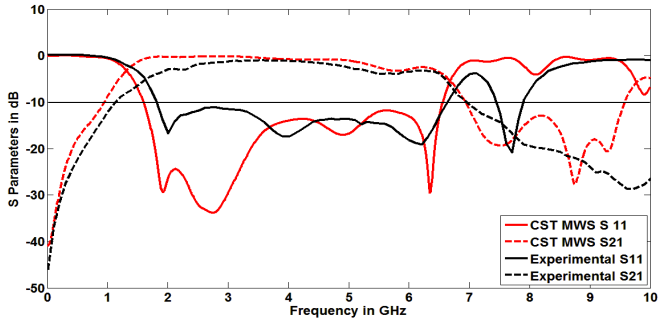

Figure 8. Simulated and experimental results of modified moore second iteration DGS filter.

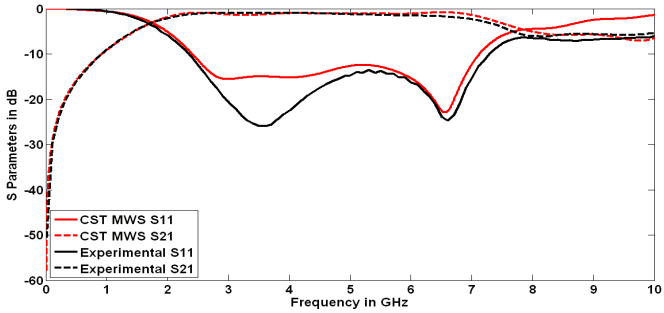

Figure 9. Simulated and experimental results of closed staircase DGS filter.

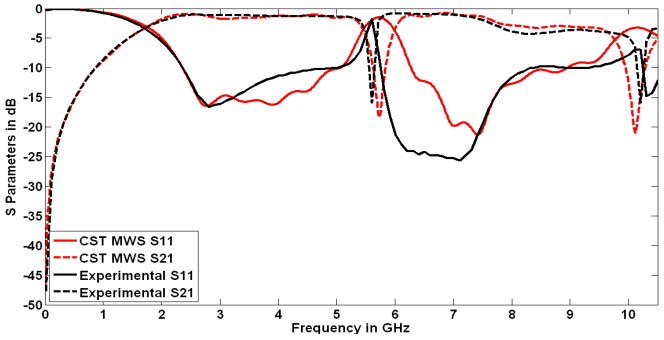

Figure 10. Simulated and experimental results of dual concentric closed staircase DGS filter.

Table 2. Performance parameters of modified moore DGS filters.

Modified Moore DGS Filter	F_L GHz		F_H in GHz		BW in GHz		Avg. S_{21} (dB)	
	Sim.	Meas.	Sim.	Meas.	Sim.	Meas.	Sim.	Meas.
First Iteration	2.24	2.27	11.38	11.86	9.14	9.59	−1.77	−2.46
Second Iteration	1.6	1.85	6.55	6.71	4.95	4.86	−1.23	−2.34

Table 3. Performance parameters of closed staircase DGS filters.

Filter Type	F_L GHz		F_H in GHz		BW in GHz		Avg. S_{21} (dB)	
	Sim.	Meas.	Sim.	Meas.	Sim.	Meas.	Sim.	Meas.
CS-DGS Filter	2.41	2.38	7.13	7.21	4.72	4.83	−1.48	−1.32
DCCS- DGS Filter (1st Band)	2.42	2.41	4.85	5.01	2.43	2.6	−1.40	−1.21
DCCS-DGS Filter (2nd Band)	6.29	5.81	8.71	8.35	2.42	2.54	−1.91	−1.84

the size of the filter effectively decreases. In terms of wavelength, first iteration has a size of $0.15\lambda_0 \times 0.15\lambda_0$ while second iteration has size $0.11\lambda_0 \times 0.11\lambda_0$, i.e., the size is reduced by 26.67%. This reduction is because of increase in the electrical length of the DGS. Another way of looking at the phenomena is that by increasing the iteration, the inductance and capacitance of the circuit increase, which decreases the lowest frequency of operation. However, it increases the Q-factor of the circuit which decreases the bandwidth. For the dual-band DCCS-DGS (Table 3), the simulated stop band (−3 dB) is from 5.56 GHz to 6 GHz with bandwidth of 0.44 GHz and isolation of −18.17 dB. The measured stop band is from 5.51 GHz to 5.82 GHz with bandwidth of 0.31 GHz and an isolation of −15.9 dB. The current distributions at the center of the pass band (also at the center of the stop band for the dual-concentric closed staircase DGS filter) for the various filters are shown in Figure 11.

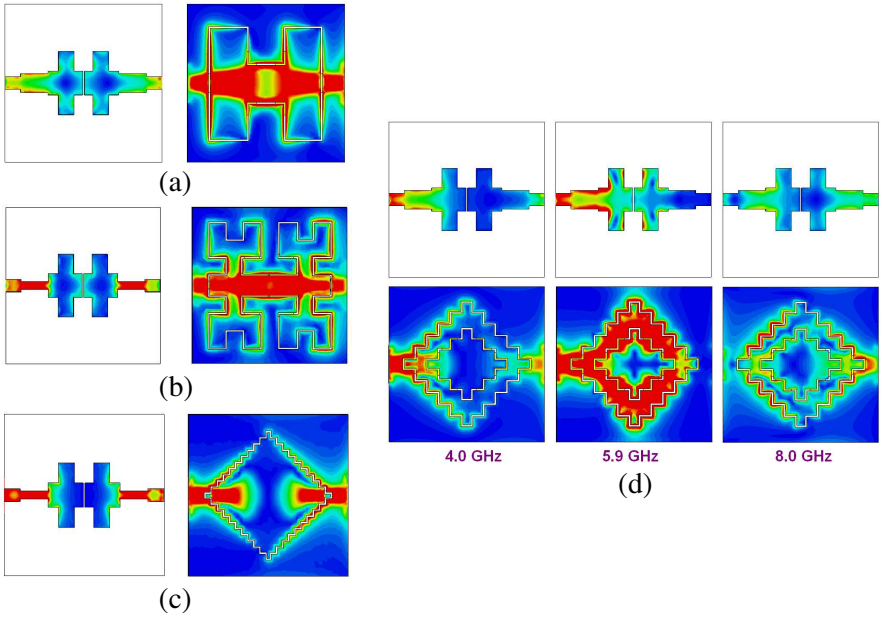

Figure 11. (a) Current distribution at 6.81 GHz for the modified moore DGS filter (1st Iteration). (b) Current distribution at 4.0 GHz for the modified moore DGS filter (2nd iteration). (c) Current distribution at 4.77 GHz for the closed staircase DGS filter. (d) Current distribution for the dual concentric closed staircase DGS filter.

5. PARAMETRIC STUDY

A stepped impedance resonator filter is simulated with different DGS geometries to assess the suitability of a given shape for the best return loss performance. The curves employed for the purpose are a square, an equilateral triangle, a circle and a hexagon, all having the same enclosed area and same slot width (Figure 12). The simulated return

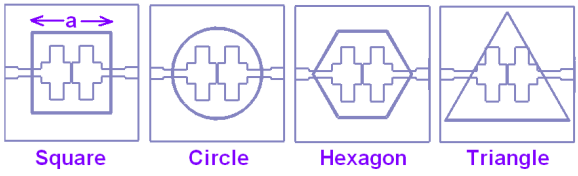

Figure 12. Different geometries for the defected ground structure.

loss obtained with various geometries is depicted in Figure 13. It can be concluded from the figure that a square slot curve gives the best performance in terms of bandwidth and impedance matching followed by the hexagon and the circle. The triangular curve results in the least bandwidth. Thus it can be inferred that slot lines with sections normal or parallel to the 50 Ω line offer better coupling of energy between the two SIR sections.

Next, the size of the defect is investigated. Filters with a square slot curve of different side lengths are simulated. The return loss

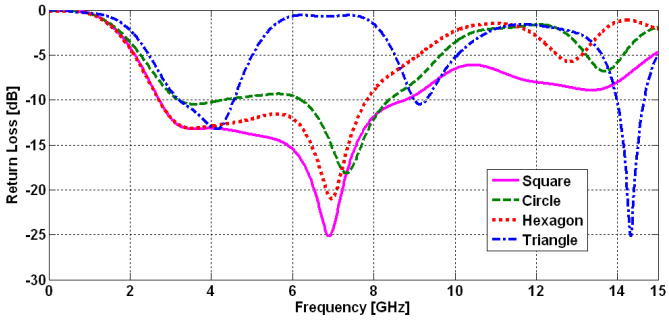

Figure 13. Effect of the shape of the DGS on the return loss of the filter.

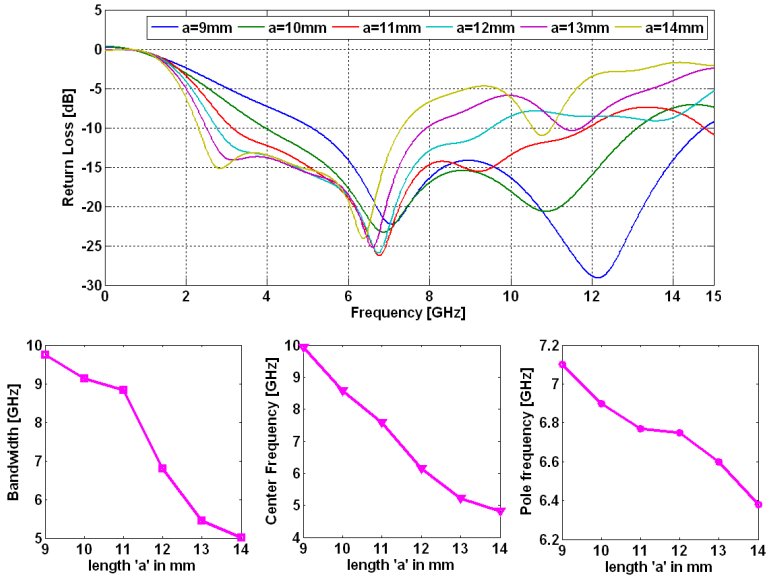

Figure 14. Effect of the side length on the return loss for the square slot DGS.

obtained for each case and the calculated parameters (bandwidth, center frequency and pole frequency) as a function of the side length 'a' are shown in Figure 14. It is observed that with an increase in the length, there is a decrease in the bandwidth along with a frequency shift to the lower side.

Finally, an empirical relation of bandwidth (BW), center frequency (f_c) and second pole frequency (f_p) relating each of these parameters to the side length of the square slot is obtained using the MATLAB curve fitting tool and given in Equations (9)–(11).

$$BW\,(\text{GHz}) = -0.061a^2 + 0.346a + 11.723 \tag{9}$$

$$f_c\,(\text{GHz}) = 0.09a^2 - 3.12a + 30.817 \tag{10}$$

$$f_p\,(\text{GHz}) = -0.0032a^2 - 0.055a + 7.82 \tag{11}$$

The above equations are specific for the SIR circuit chosen in the present study and for a substrate relative permittivity of 2.2 and thickness of 0.508 mm. In what follows, results of parametric studies for the different filters (Modified Moore Curve DGS, Closed Staircase DGS, Dual Concentric Closed Staircase DGS) are presented.

5.1. Modified Moore Curve (1st Iteration) DGS Filter

5.1.1. Size of the Grid

A parametric study was done by scaling the Modified Moore curve (1st Iteration) etched on the ground plane in order to study its effect on the resonant frequencies and bandwidth. The shape can be visualized to be inscribed in a square of side G. So, scaling can be represented by the change in G. The effect of changing G on S_{11} curve is shown in Figure 15.

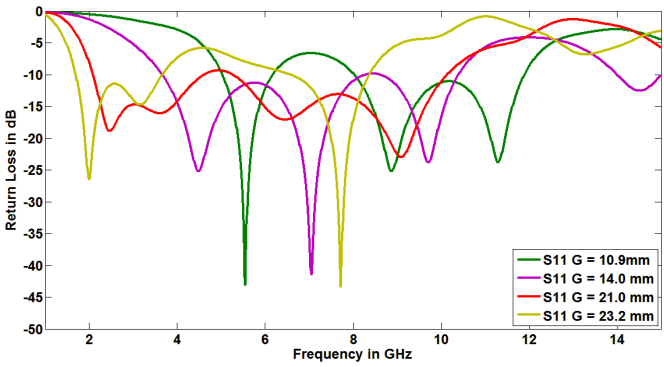

Figure 15. Effect of variation of grid size on S_{11} (modified moore — first iteration DGS filter).

It can be seen that when the size is smaller, the pass band starts at higher frequency, and as the size increases, it shifts to a lower value. This is due to an increase in the length of the curve with an increase in the size of the square. Also, with varying size, different parts of the SIR circuit come in proximity with the DGS, which affects the impedance matching. Overall, there exists an optimal value for which the entire pass band has $S_{11} < -10$ dB.

5.1.2. Effect of the Width of the 2nd Segment of Stepped Microstrip Line

For obtaining good bandwidth, optimization of the microstrip SIR circuit printed on the top plane is required. In this respect, parametric analysis for the width of the various segments of the SIR is done. It is found that the width of segment M2 (Figure 3(a)) governs the impedance around 5 GHz and hence is crucial in obtaining good impedance matching over the desired bandwidth. Figure 16 shows the effect of varying the width of M2 on return loss and insertion Loss.

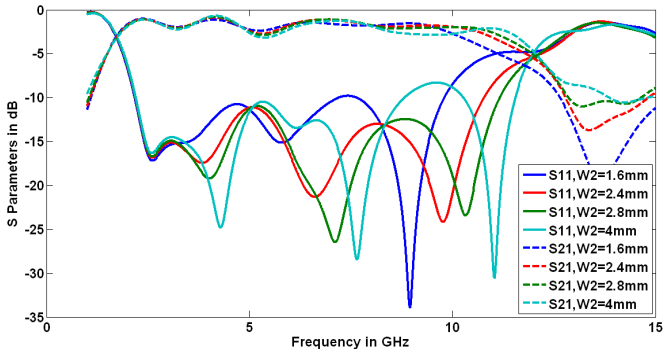

Figure 16. Parametric study for the width of 2nd segment of stepped microstrip line (modified moore — first iteration DGS filter).

It can be observed from the figure that as the width of the segment M2 is varied from 1.6 mm to 4 mm, we get different -10 dB bandwidths ranging from 7.63 GHz to 9.31 GHz. From the parametric study, it can be concluded that when the value of the width of M2 is put at 2.4 mm, the widest bandwidth of 9.14 GHz is obtained.

5.1.3. Effect of the Slot Width

An increase in slot width results in a lower frequency of operation. It can be observed from Figure 17 that as the slot width of the ground

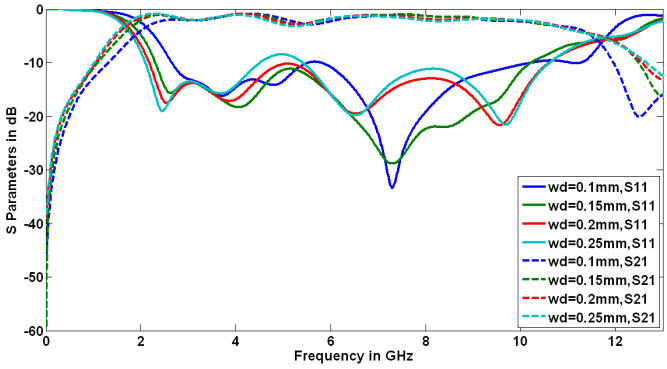

Figure 17. Parametric study for the slot width (Wd) (modified moore — first iteration DGS filter).

defect is increased, the bandwidth also increases. As the slot width (Wd) is varied from 0.1 mm to 0.25 mm, we get improved bandwidths from 9.56 GHz to 10.28 GHz. The value of 0.2 mm for Wd is observed to give the ultra wide bandwidth of 10.28 GHz.

5.1.4. Effect of the Gap between Resonators 'S'

The effect of varying the gap between the two SIR sections denoted by 'S' (Figure 3(a)) is shown in Figure 18. The gap is varied from 0.1 mm to 0.5 mm, and both the return loss and insertion loss are calculated. From the figure, it is seen that practically, there is no effect on the lower

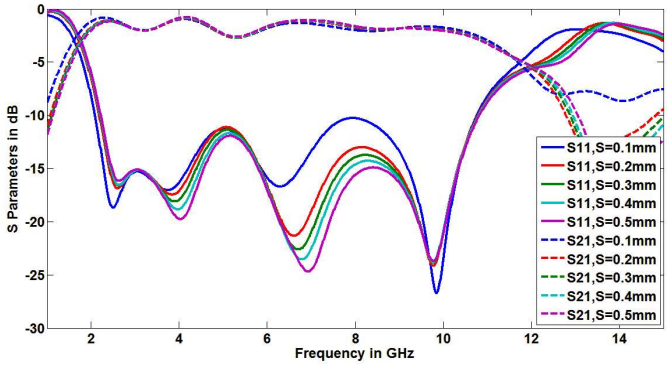

Figure 18. Effect of the gap between SIR sections 'S' on return and insertion loss (modified moore — first iteration DGS filter).

and upper cut off frequencies, i.e., the bandwidth remains the same. However, the impedance matching improves at higher frequencies with a larger gap accompanied by a slight shift in the resonances.

5.2. Closed Staircase DGS Filter

5.2.1. Effect of Various Iterations

The effect of increasing the iterations on the performance of the closed staircase — defected ground filter is shown in Figure 19. An improvement in the performance due to better impedance matching is clearly observable with an increase in the number of iterations. However, the improvement reduces at higher iterations, and hence the 11th iteration with the best return loss performance was chosen for fabrication.

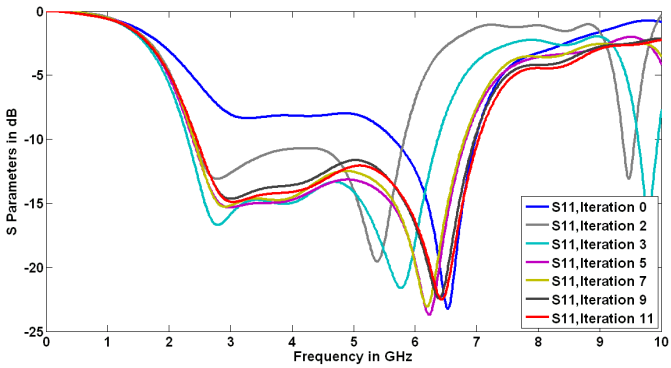

Figure 19. Effect of iteration number on performance of closed staircase DGS filter.

5.2.2. Effect of Variation in Size of Defect ($D1$)

The size of the structure traced by the slot on the ground plane plays a crucial role in structuring the inductance and capacitance of the filter which in turn determine the cut-off frequencies as well as the Q or bandwidth of the circuit. In order to study the effect of the size of the closed staircase structure on the return loss, the parametric study was performed by varying the dimension $D1$ (Figure 3(c)), and the results are plotted in Figure 20.

It can be observed from the figure that as slot dimension $D1$ is varied from 9.45 mm to 18.9 mm, different bandwidths from 0.73 GHz to 4.21 GHz are obtained. Initially, the bandwidth increases as $D1$

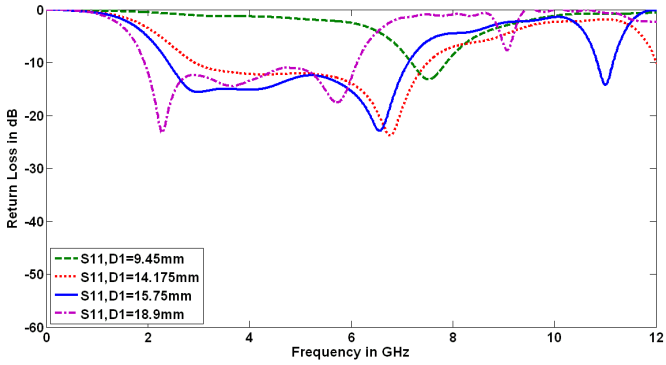

Figure 20. Parametric study for the slot dimension $D1$ (closed staircase DGS filter).

is increased and thereafter decreases. It is also observed that with an increase in $D1$, the resonance frequencies shift towards the lower side. After optimization of the proposed structure, the value of $D1$ is taken 15.75 mm for fabrication which gives the widest bandwidth of 6.06 GHz.

5.2.3. Effect of Width of 2nd Segment of Stepped Microstrip Line

As for Modified Moore curve DGS filter, the width of the segment M2 is crucial in obtaining good impedance matching over the desired bandwidth. The variations in the return loss for different sizes of M2 for the closed staircase DGS filter are shown in Figure 21. The width of M2 is varied from 0.5 mm to 2.0 mm, and different -10 dB bandwidths from 1.85 GHz to 4.5 GHz are obtained.

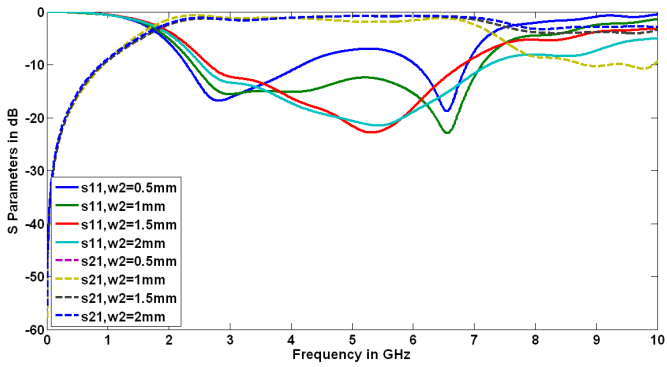

Figure 21. Parametric study for the width of the 2nd segment of stepped microstrip line (closed staircase DGS filter).

5.2.4. Effect of Ground Slot Width

As the slot width increases, the lower frequency of operation decreases, and the bandwidth increases. It can be observed from Figure 22 that as the slot width in the defected ground is increased from 0.1 mm to 0.25 mm, we get different improved bandwidths from 2.33 GHz to 5.09 GHz.

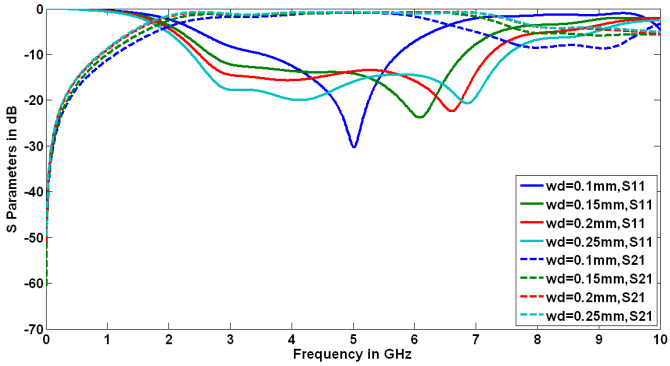

Figure 22. Parametric study for the ground slot width (closed staircase DGS filter).

5.3. Dual Concentric Closed Staircase DGS Filter

5.3.1. Effect of Width of 2nd Segment of Stepped Microstrip Line

At first, the effect of varying the size of M2, the second segment of the SIR (Figure 3(d)) is studied. The widths are varied from 1 mm to 3.4 mm, and we get different bandwidths from 1.31 GHz to 3.61 GHz for the first band and from 0.28 GHz to 3.51 GHz for the second band (Figure 23). It is also observed that as the width of M2 increases, the bandwidth of first band decreases, and that of second band increases. The optimum value of width of M2 is found to be 3.4 mm. The width of M2 can be used to control the bandwidths of the two bands of the filter.

5.3.2. Effect of Slot Width and Gap between SIR Sections

The effect of increasing the ground slot width on the return loss and insertion loss of the dual concentric closed staircase DGS filter is shown in Figure 24. It is seen that, with an increase in the slot width, the lower cut off frequency decreases, and the bandwidth increases. As the

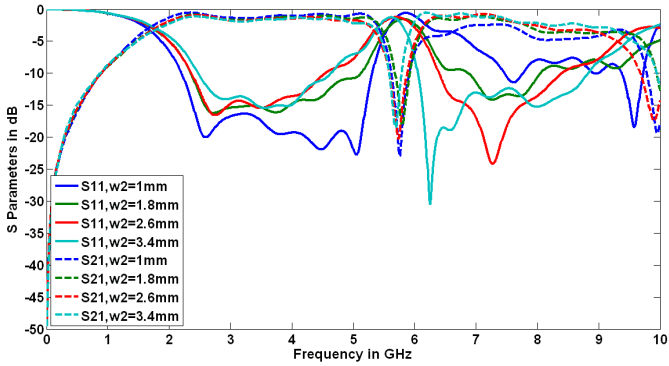

Figure 23. Parametric study for the width of 2nd segment of stepped microstrip line of dual concentric closed staircase DGS filter.

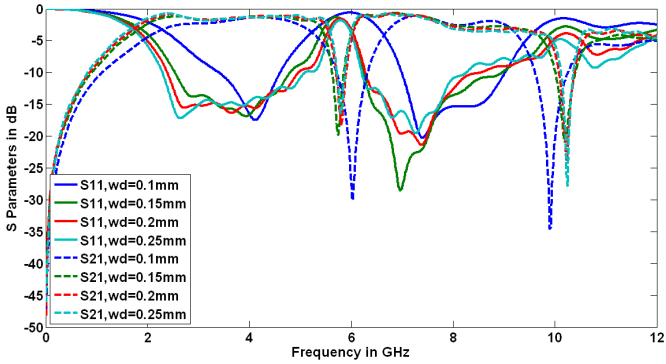

Figure 24. Parametric study for the ground slot width of the dual concentric closed staircase DGS filter.

slot width (Wd) is varied from 0.1 mm to 0.25 mm, we get different improved bandwidths from 1.32 GHz to 2.99 GHz for the first band and from 2.04 GHz to 2.14 GHz for the second band. The effect of the gap between the SIR sections is shown in Figure 25 from which no significant variations are observed in either the return loss or the insertion loss with a change in the gap.

The effect of simultaneous variation of the width of the second step of the stepped impedance resonator '$W2$' and the width of the slot in the ground plane 'Wd' is shown in Figure 26. The bandwidth obtained ($S_{11} < -10$ dB) as a function of the SIR width '$W2$' for different values of slot width 'Wd' is plotted in Figure 27. From Figure 26, it can be observed that, in general, an increase in the slot width and

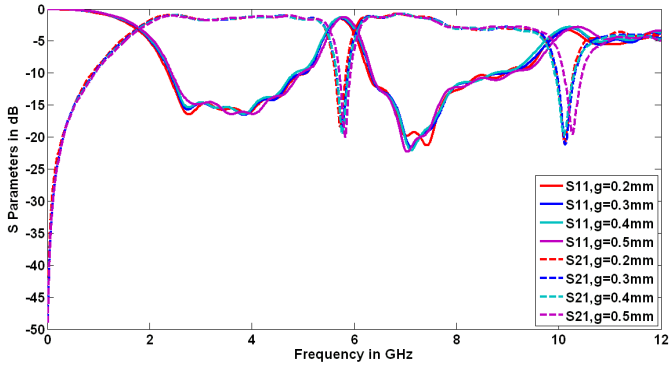

Figure 25. Effect of the gap between SIR sections 'S' on return and insertion loss for the dual concentric closed staircase DGS filter.

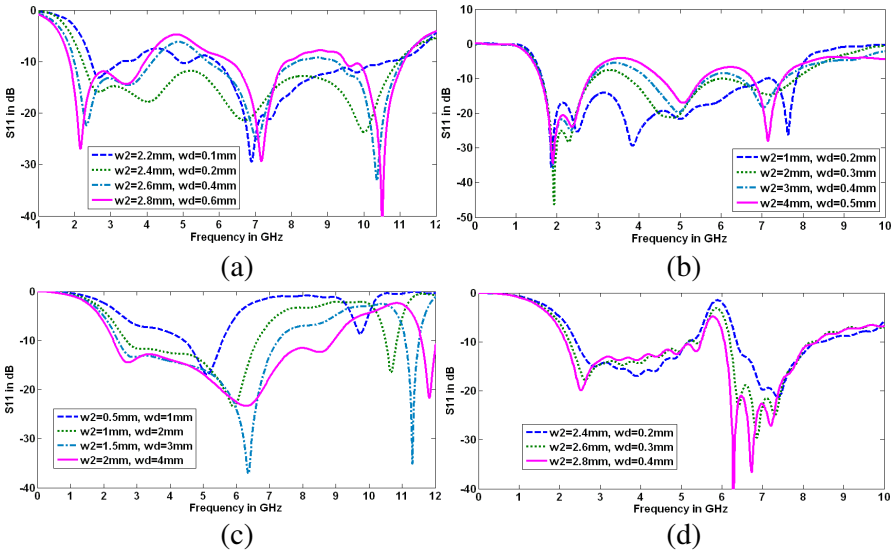

Figure 26. Effect of simultaneous variation of microstrip line width '$w2$'. and slot width 'wd' on the return loss of various filters. (a) Modified moore DGS filter (1st Iteration). (b) Modified moore DGS filter (2nd Iteration). (c) Closed staircase DGS filter. (d) Dual concentric closed staircase filter.

$W2$ leads to a lower cut-off frequency F_L and improved matching over certain frequencies. From Figure 27, it is seen that the bandwidth obtained increases with the slot width and varies uniformly with the SIR width $W2$ (except for Modified Moore — 2nd iteration) over the

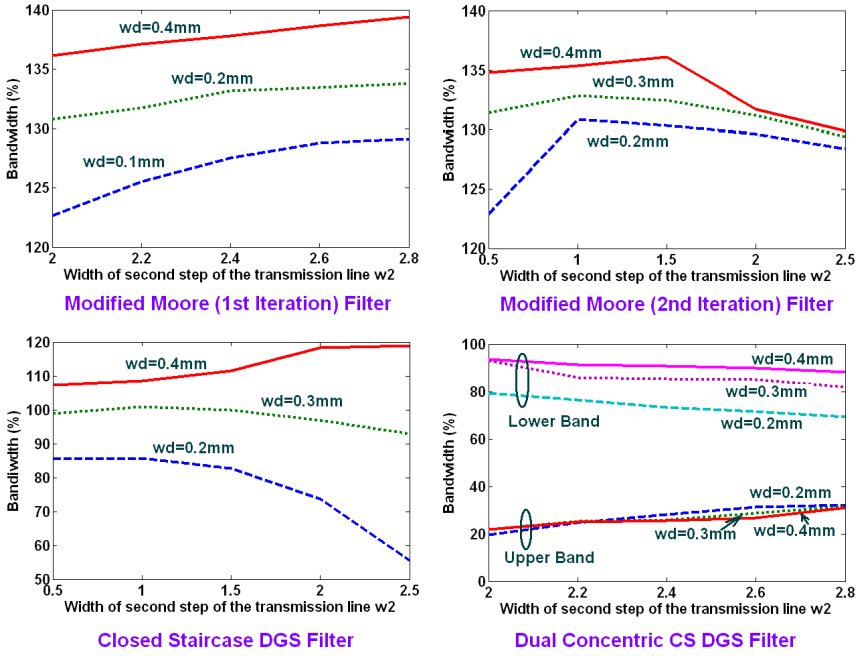

Figure 27. Bandwidth obtained (-10 dB of S_{11}) as a function of microstrip width '$W2$' for different values of slot width 'Wd'.

chosen values. However, it is noted that the bandwidth depicted in Figure 27 is meant to show a trend and does not necessarily imply a good impedance matching throughout the band as evident from Figure 26 where the mismatch increases over certain bands. Further, a change in the slot width may change the slope of the bandwidth variation as seen for the closed staircase filter. The indication of optimized values for the parameters is thus evident.

6. CONCLUSION

Four different band-pass filters utilizing stepped impedance resonator and defected ground structures are proposed. The geometries employed for the DGS are the Modified Moore fractal (first and second iterations), closed staircase and dual-concentric closed staircase. The H-shape structure (Modified Moore — first iteration) operates from 2.27 GHz to 11.86 GHz with a bandwidth of 9.59 GHz covering ISM and UWB specifications. The Modified Moore 2nd iteration operates from 1.85 GHz to 6.71 GHz with the bandwidth of 4.86 GHz. The

closed-staircase structure operates from 2.38 GHz to 7.21 GHz with the bandwidth of 4.83 GHz. The dual-concentric closed-staircase structure operates in dual bands, from 2.41 GHz to 5.01 GHz with the bandwidth of 2.60 GHz and 5.81 GHz to 8.35 GHz with the bandwidth of 2.54 GHz. Parametric studies indicate that size of the slot in the ground affects the cut-off frequencies as well as the bandwidth of the filters. In case of the dual-concentric closed-staircase DGS filter, the structure can be tuned to obtain a response ranging from single wideband to dual band with individual bandwidths depending on the size of the slot. Also it is seen that the width of the segments in the stepped impedance resonator can be tuned to obtain better impedance matching in the desired frequency band. The designed filters have simple planar structures with compact size, wider bandwidth and are easy to fabricate.

ACKNOWLEDGMENT

The authors thank the reviewers for their useful suggestions. They would also like to thank the Vice Chancellor, DIAT, Girinagar, Pune for the financial support and encouragement and the research students at the Microwave and Millimeter wave Antenna Lab, DIAT for their support.

REFERENCES

1. Jaldi, M. and M. Tayarani, "Characteristics of a novel slow-wave defected ground structure for planar wideband filters," *International Conference on Information and Electronics Engineering IPCSIT*, Vol. 6, Singapore, 2011.
2. Liu, H. W., Z. C. Zhang, X. H. Guan, and S. Jiang, "A bandpass filter based on fractal shaped defected ground structure resonators for wireless communication," *2010 International Conference on Microwave and Millimeter Wave Technology (ICMMT)*, 201–203, 2010.
3. Huang, J.-F., J.-Y. Wen, and M.-C. Huang, "Design of a compact planar UWB filter for wireless communication applications," *International Conference on Wireless Communications & Signal Processing, WCSP 2009*, 13–15, Nov. 2009.
4. Jarry, P., J. Beneat, and E. Kerherve, "Fractal microwave filters," *2010 IEEE 11th Annual Wireless and Microwave Technology Conference (WAMICON)*, Vol. 1, No. 5, Apr. 12–13, 2010
5. Xiao, J.-K., Q.-X. Chu, and S. Zhang, "Novel microstrip triangular resonator bandpass filter with transmission zeros

and wide bands using fractal shaped defection," *Progress In Electromagnetics Research*, Vol. 77, 343–356, 2007.

6. Chen, J., Z.-B. Weng, Y.-C. Jiao, and F.-S. Zhang, "Lowpass filter design of Hilbert curve ring defected ground structure," *Progress In Electromagnetics Research*, Vol. 70, 269–280, 2007.
7. Patin, J. M., N. R. Labadie, and S. K. Sharma, "Investigations on an H-fractal wideband microstrip filter with multi-passbands and a tuned notch band," *Progress In Electromagnetics Research B*, Vol. 22, 285–303, 2010.
8. Xu, H.-X., G.-M. Wang, and Q. Peng, "Fractal-shaped complementary electric-LC resonator for bandstop filter," *Progress In Electromagnetics Research C*, Vol. 23, 205–217, 2011.
9. Kim, I. K., N. Kingsley, M. Morton, R. Bairavasubramanian, J. Papapolymerou, M. M. Tentzeris, and J.-G. Yook, "Fractal shaped microstrip coupled line band pass filters for suppression of second harmonic," *IEEE Transactions on Microwave Theory and Techniques*, Vol. 53, No. 9, Paper No. 2898, 2943–2948, 2005.
10. Ali, J. K. and H. Alsaedi, "Second harmonic reduction of miniaturized dual-mode microstrip band pass filters using fractal shaped open stub resonators," *PIERS Proceedings*, 1266–1269, Kuala Lumpur, Malaysia, Mar. 27–30, 2012.
11. Taher, H. M., "A simplified equivalent circuit model for defected ground structures in planar transmission lines," *Progress In Electromagnetics Research Letters*, Vol. 29, 157–166, 2012.
12. Guo, Y. H. and Q. Wang, "An improved parameters extraction method for dumbbell shaped defected ground structure," *Engineering*, Vol. 2, No. 3, 197–200, 2010.
13. Breed, G., "An introduction to defected ground structures in microstrip circuits," *High Frequency Electronics*, 50–52, Nov. 2008.
14. Chaudhary, G., P. Kim, Y. Jeong, J. Lim, and J. Lee, "Analysis and circuit modeling method for defected microstrip structure in planar transmission lines," *Proc. Asia-Pacific Microwave Conference 2011*, 999–1002, 2011.